



Arsenic in the waters and sediments of the Humboldt River, North-Central Nevada, USA: hydrological and mineralogical investigation

Shahnewaz Mohammad¹ · Regina N. Tempel^{1,2}

Received: 3 April 2019 / Accepted: 12 August 2019 / Published online: 24 August 2019
© Springer-Verlag GmbH Germany, part of Springer Nature 2019

Abstract

Arsenic (As) concentration in the Humboldt River (HR) water ranges from 0.012 to 0.06 mg/L, with an average of 0.032 mg/L. The river water is alkaline with pH 8.4–9.3 and oxic with average 12 mg/L of dissolved O₂ and + 139 mV of oxidation–reduction potential (ORP). The river water contains an average specific electrical conductivity of 1000 µS/cm with elevated B (average 0.77 mg/L), Li (average 0.15 mg/L), Cl (average 158 mg/L), and SO₄ (average 178 mg/L). Factor analysis of river water chemistry and sediment chemistry suggests several physical and geochemical processes operating in three sub-regions: upper, middle and lower reaches of the river. Oxidative dissolution of As-bearing sulfide minerals in the upstream is the primary source of As to the water. Groundwater–surface water interactions affect As concentrations in localized area between the middle and lower HR. Further enrichment of As occurs by evaporation in the lower reach and the terminal sink of the river. Results of sequential extraction analysis and scanning electron microscopy (SEM) of the riverbed sediments suggest that As distribution in the river sediments is controlled by partitioning to clay minerals and Fe-oxy-hydroxides.

Keywords Arsenic · Humboldt River · Nevada · Oxidation · Ferrihydrite · Clay minerals

Introduction

The Humboldt River (HR) is the largest internally drained river in Nevada, and with approximately 43,700 km², the Humboldt River Basin (HRB) is a substantial part of the Great Basin (Fig. 1). The HRB hosts various metallic and non-metallic economic deposits and is a leading producer of gold, silver, copper, mercury and tungsten in the US (Wallace et al. 2004). The HR and the basin play important roles

in providing valuable sources of water for mining, construction, power plants, and municipal water supply.

Previous studies reported elevated concentrations of dissolved arsenic (As) in several river waters surrounding the HRB, including Carson River (5–175 µg/L), Walker River (< 2–135 µg/L) (Johannesson et al. 1997) and North Fork-Humboldt River (4–12 µg/L) (Earman and Hershey 2004). Arsenic in these river waters has been accounted for with weathering of geologic materials, hydrothermal sources and drainage through mined waste rocks, but there have been no studies on As occurrences in the HR waters. This study is a first of its kind with broad hydrological and geochemical analysis for the HR water and sediments to understand the processes controlling As distribution between the sediments and waters of the HR.

Electronic supplementary material The online version of this article (<https://doi.org/10.1007/s12665-019-8552-1>) contains supplementary material, which is available to authorized users.

✉ Shahnewaz Mohammad
mshahnewaz@gmail.com

Regina N. Tempel
gtempel@unr.edu

¹ Graduate Program of Hydrologic Sciences, University of Nevada, Reno, NV, USA

² Department of Geological Sciences and Engineering, University of Nevada, 1664 N Virginia St, Reno, NV 89557, USA

Study area description

The HR with its tributaries, the Little Humboldt River and the Reese River, flows west and then south–west into the Humboldt Sink (Fig. 1) forming three geographic subdivisions of the HR system: Upper Humboldt River (UHR),

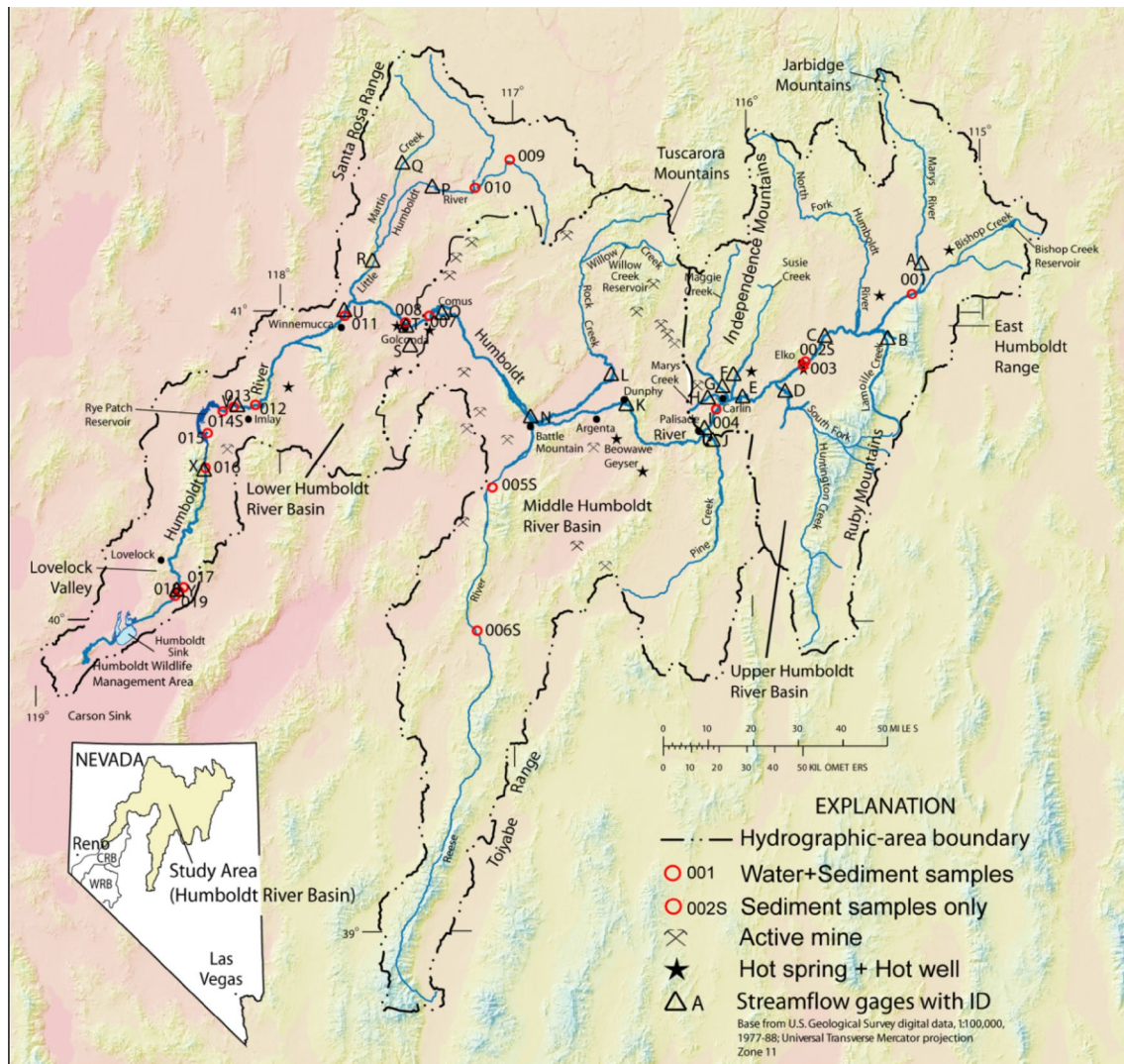


Fig. 1 Map of the Humboldt River Basin (HRB) in northern Nevada showing the Humboldt River and locations of sampling points of river water and sediments. The inset map shows the study area with

locations of Carson River Basin (CRB), Walker River Basin (WRB) on the south–west of the HRB

Middle Humboldt River (MHR), and Lower Humboldt River (LHR).

The UHR extends from its source at the base of the East Humboldt Range, Ruby Mountains, and Jarbidge Mountains to the confluence of Susie Creek and Maggie Creek near Carlin (Fig. 1). Miocene volcanic and sedimentary rocks with some pre-Tertiary volcanic rocks are widespread in this area with lesser extent of the Quaternary sediments.

The MHR between Carlin and Comus (Fig. 1) contains relatively widespread Tertiary volcanic and Cenozoic sedimentary rocks in the east of Battle Mountain, and widespread Quaternary alluvium and lacustrine deposits in the west of Battle Mountain.

The LHR between Comus and the Humboldt Sink (Fig. 1) consists of Quaternary alluvium and playa deposits, lake evaporites and lacustrine deposits.

Hydrogeologic framework

The average annual precipitation in the HRB is 21–35 cm. The average monthly evaporation for shallow open water is 10.4–11.4 cm in the UHR and MHR regions, and about 11.6–12.7 cm around Imlay, Winnemucca, Rye Patch Reservoir and Lovelock area in the LHR region. The rate of evaporation in the LHR is higher than in the UHR and MHR, and is consistent with the availability of more surface areas and open waters in the LHR. Tables A.1 and

A.2 (in Online Appendix A) provide data for precipitation (SNDWR 2019) and potential evapotranspiration (PET) data (NCEI 2019).

The shallow groundwater in the HRB occurs under water-table conditions during most of the year, with some artesian conditions occurring locally, where impermeable clay units overlie the saturated units. Several thermal springs occur in relatively small areas locally, where water occurs under artesian conditions. The river was in low-flow condition relatively during the sampling period in September 2007. During the low-flow season, gains and losses occur largely by the interchange of water between the river and the ground water reservoir, whereas increases in base flow during fall and winter result from seasonal reductions of PET loss. Previous studies indicate that direct infiltration of precipitation contributes only a small part of the average annual ground water recharge, and the source of the most ground water is seepage from stream flow, where the ultimate source of the stream flow is precipitation (Prudic et al. 2007).

Methods and materials

The location of water and sediment samples sites along with locations of active mines and hot springs are illustrated in Fig. 1. Because of the large extent of study area and limited accessibility of some locations, multiple samples at the intersection of highways and the river were collected. A total of fifteen (15) water samples and eighteen (18) sediment samples were collected along the HR with multiple numbers of samples at each location. The samples were then weighted for average for each location. The sediment samples from the riverbeds were collected using an extensional hand auger at depths of 1.5–2 m beneath the riverbed.

Analytical methods for river water

Following on site measurement, the water samples were collected using a 0.45- μm filter and preserved according to the US Geological Survey sampling protocol (Shelton 1994) to ensure the quality-assurance/quality-control (QA/QC). A subset of samples was acidified with concentrated reagent-grade HNO_3 for trace metals and major cations analysis. Inductively Coupled Plasma-Mass Spectrometer (ICP-MS) was used to analyze major cations and trace elements. Ion Chromatography was used to analyze major anions from another subset of samples. The QA/QC was achieved by analyzing replicates, filled blank solutions, and certified reference solutions, where the computed charge balance was $\leq 5\%$. Table 1 lists the physical and chemical components of water samples from the HR.

Stable isotope analysis of δD (deuterium) and $\delta^{18}\text{O}$ (oxygen-18) was performed following Morrison et al. (2001) and

the $\text{CO}_2\text{-H}_2\text{O}$ equilibration methods of Epstein and Mayeda (1953), respectively, using Micromass Iso Prime (MIP) stable isotope ratio mass spectrometer. Dissolved sulfate- $\delta^{34}\text{S}$ (sulfur-34 of dissolved sulfate) analysis was performed by precipitating dissolved sulfate as BaSO_4 following Carmody et al. (1998) using a Eurovector elemental analyzer interfaced to a MIP stable isotope ratio mass spectrometer. The results of δD and $\delta^{18}\text{O}$, and $\delta^{34}\text{S}$ are reported in units of ‰ against the VSMOW and VCDT standards, respectively, with an uncertainty of $\pm 0.1\text{‰}$ (Table 1).

Analytical methods for river sediments

The sediment samples were dried at room temperature, disaggregated and crushed with acetone-washed porcelain pestle and mortar, and then sieved through a nylon 80 mesh ($< 170\ \mu\text{m}$). These screened sediment samples were used for sequential extraction. The extractions were performed in constantly agitated 50-ml centrifuge tubes, with a sample size of 1 g following modified methods of Tessier et al. (1979) and Li et al. (1995). After each extraction stage, supernatant was separated from the residue by centrifugation, and was stored into polypropylene bottles for analysis. The residue was rinsed twice with deionised water, hand-shaken and separated by centrifugation. The sequential extraction separated in the order of exchangeable metals, carbonate-bound metals, amorphous Fe–Mn oxide metals, organic metals, and residual fractions. Finally, total metals were extracted by digesting 400 mg of samples with 8-ml aqua-regia to determine the initial contents. All extracted fractions were analyzed using ICPMS for concentrations of total elements. The sum of elemental concentrations in each fraction and the inaccessible residual fraction is equal to initial content within the experimental error of $\pm 3\%$. Table B.1 (Online Appendix B) lists the sequential extraction analysis results.

Selected samples that contained high and low concentrations of arsenic in the sequential extraction were further analyzed by X-ray powder diffractometry (XRD) and Scanning Electron Microscopy (SEM) to determine the mineralogical associations in the sediments. XRD analysis was conducted using a Cu $\text{K}\alpha$ radiation and a graphite monochromator on a Philips[®] vertical diffractometer, stepped at 0.03, from 2° to 60° diffraction angle (2θ). Identification of the minerals in the samples was conducted using PC-APD[®] Diffraction software of Philips Analytical with search/match of the reference mineral database and generated powder patterns. SEM analysis was conducted using a Hitachi S-4700 field-emission scanning electronic microscope. SEM is a qualitative method for high-resolution imaging of surfaces using electrons for imaging with the advantage of much higher magnification ($> 100,000\times$) and greater depth of field up to 100 times that of light microscopy. Quantitative chemical

Table 1 Summarized physical parameters and chemical components of waters from the Humboldt River

Sample ID	PH	ORP (mV)	Cond. (μS)	Temp ($^{\circ}\text{C}$)	Ca	Mg	Na	K	Cl	SO ₄	Alk	B	Li	Fe	Mn	SiO ₂	As	$\delta^{18}\text{O}$	δD	$\delta^{34}\text{S}$
U 001	8.77	125.6	1240	14.7	75.9	70.03	252	18.47	61.5	565.1	525.82	2.13	0.11	<0.01	0.01	15.9	0.066	-14.5	-114	4.7
H 003	8.64	134.5	760	18.5	125	57.12	301.3	17.54	151.4	566.3	440.42	0.84	0.29	<0.01	0.37	20.7	0.012	-15.1	-125	9.8
R 004	8.85	10	720	17.6	49.1	20.38	47.99	10.53	24.3	59.3	264.74	0.24	0.11	0.02	0.06	14.8	0.013	N.S.	N.S.	10.3
007	8.85	105	980	13.6	57.9	29.35	173.7	11.91	120.6	144.1	420.9	0.52	0.10	0.04	0.00	15.2	0.021	-9.4	-98	12
008	8.85	105.4	920	16.2	47.7	19.19	146.4	11.76	75.1	104.6	347.7	0.64	0.17	0.03	0.00	18.2	0.037	-11.6	-105	N.S.
009	8.91	143.4	680	14.6	37.3	6.99	50.01	10.88	24	28.9	195.2	0.20	0.03	0.03	0.01	17.3	0.015	-9.2	-92	N.S.
010	8.44	162.6	660	17.4	29.2	5.68	63.21	13.04	26.7	32.4	195.2	0.22	0.04	0.01	0.01	40.4	0.012	-15.7	-125	N.S.
L 011	8.55	156.1	780	13.8	67.8	20.67	139.4	10.05	88.8	124.8	418.46	0.51	0.09	0.01	0.46	22.9	0.017	-13.9	-115	N.S.
H 012	8.96	192.4	830	9.9	43	24.05	114.4	8.92	108.7	132.1	276.94	0.69	0.08	0.03	0.01	14.9	0.019	-12.6	-110	N.S.
R 013	8.95	168	840	11.4	38.7	26.95	133	10.76	123	146.9	235.46	0.80	0.08	0.01	0.00	12.4	0.022	-11.1	-103	N.S.
015	9.13	139.3	1020	17.8	37.4	22.68	168.4	18.17	134.1	124.8	342.82	0.54	0.17	0.02	0.00	16.0	0.048	-7.5	-85	7.2
016	9.25	125	980	17.6	37.9	21.46	148.6	15.68	111.6	98.6	323.3	0.47	0.13	0.01	0.00	15.8	0.037	-8.5	-89	N.S.
017	9.04	145.2	1080	14.5	46.2	20.73	307.6	26.33	332.1	141.5	409.92	1.22	0.30	0.02	0.00	18.5	0.048	-9.6	-95	N.S.
018	8.92	136.1	1160	13.9	42.6	21.55	422.6	27.98	508.6	162.6	427	1.29	0.26	0.03	0.00	19.4	0.053	-9.6	-94	N.S.
019	8.93	119.2	1280	14.5	43.7	21.53	417.9	28.32	481.5	159.3	392.84	1.23	0.26	0.03	0.00	20.2	0.052	-9.7	-94	N.S.

Concentrations are in mg/L unless otherwise stated. Concentrations of arsenic are reported as total As

ORP oxidation–reduction potential, Alk alkalinity as HCO_3^- ; stable isotopes in ‰; NS no sample. NO_2^- , NO_3^- , and PO_4^{3-} were below detection limit

analysis information was obtained using an energy-dispersive X-ray spectrometer (EDS) with the SEM to determine the mineralogical composition. The EDS technique detects X-rays emitted from the sample during bombardment by an electron beam to characterize the elemental composition of the analyzed volume. With EDS, features or phases as small as 1 μm or less can be analyzed.

Data analysis

The data were investigated using two approaches. First, the data were investigated to determine the geochemistry and evolved water chemistry by applying qualitative geochemical tools such as Piper diagrams and Stiff diagrams. Second, the relationship of As with various geochemical parameters was investigated by applying statistical factor analysis method.

Factor analysis is useful in determining the major processes that may control the distribution of hydro-chemical variables and many researchers have used this method in similar studies (Wang et al. 2007; Dongarrà et al. 2009; Jang 2010). These statistical calculations were performed by applying Principal Component Analysis (PCA) solution to the factor analysis model. The PCA represents the covariance structure of the data using a set of new uncorrelated variables that are obtained as linear combinations of the initial variables in a way that maximizes the variance of individual new variables. The resulting factor loadings, also known as component loadings in PCA, are the covariance between the variables and factors. Analogous to Pearson's r , the squared factor loading is the percent of variance in that indicator variable (i.e., chemical parameters) explained by the factor.

Assumptions and limitations for factor analysis

The basic assumption in factor analysis is that the variables are linearly related. Because the factor analysis method is based on the covariance or correlation matrix, the results are influenced by the similarities between samples, and consequently can be affected by extreme outliers or inadequate data sets (Davis 2002).

One of the primary limitations of the factor analysis method is that it is often difficult to determine the optimal solution and thus the number of factors to retain in the final solution. Therefore, a more philosophical assumption is required that the underlying factors extracted from the data set represent physically meaningful processes. In practice, the number of factors used in factor analysis equals the number of Eigenvalues of the correlation matrix that is larger

than one, because the sums of squares are normalized to unit variance; the magnitude of the Eigenvalues provides a measure of their importance relative to the original variables (Davis 2002).

In this study, the first step of factor analysis involved standardizing the raw data by converting them into dimensionless variables. Then, the data were transformed into factors followed by determination of correlation matrix, Eigenvalues and eigenvectors to yield the covariance matrix. Resultant factors with Eigenvalues exceeding one were retained. Further, the factors with higher Eigenvalues that are separated by wide margins from each other were accepted as meaningful factors (Reyment and Joreskog 1996). In this study, the absolute value of factor loading 0.5 is used as a cutoff value following similar studies (Wang et al. 2007). The terms, "strong" "moderate" and "weak" as applied to factor loadings, refer to absolute values of >0.75 , $0.75-0.5$, and $0.5-0.3$, respectively. All statistical data analyses were performed using SPSS version 21.0 (IBM Corp 2012).

Groundwater–surface water interaction analysis

Because of the importance of groundwater–surface water interactions, the base flow was analyzed using a simple web-based method called WHAT (Web Based Hydrograph Analysis Tool 2019; <https://engineering.purdue.edu/mapserve/WHAT/>) to determine the fractions of direct runoff and groundwater inflows from the stream-flow data (Table 2). The assumptions used in this calculation are as follows: (1) the streams are intermittent with porous aquifer materials, (2) the total stream flow equals the summation of direct runoff and base flow, (3) direct runoff equals the rainfall excess. The direct runoff is defined as follows: $\text{direct runoff} = \text{rainfall} - \text{losses}$, where losses = interception, infiltration, depression storage, etc., also known as basin recharge; and $\text{rainfall excess or direct runoff} = \text{overland flow}$. The ratio of total base flow to discharge is base flow index (BFI).

The BFI indicates that the majorities of flows were due to base flow, which is consistent with a relatively dry season during sampling. The base flow is 100% and 97% for instance, at locations near samples 001 and 003, respectively (Table 2).

The total flow of the HR increases between Carlin and Palisade as illustrated in Table 2, despite very low flows in Susie Creek, Maggie Creek and Mary's River. In as much as virtually no surface water discharged into this reach of the river, nearly the entire increase in the flow during this low flow period is the result of ground water discharging into the river. Similarly, with virtually no flow at Comus, the increase in flow at Imlay is due to subsurface inflow of ground water discharging into the river.

Table 2 Average daily base flow and total flow of the Humboldt River during August–September, 2007. Data source: <http://wdr.water.usgs.gov/>

Abbreviated ID* (Sample #)	USGS station ID	Stream gage location name	Total flow (m ³ /s)	Direct runoff (m ³ /s)	Base flow (m ³ /s)	BFI
A (001)	10315600	MARYS RV BLW TWIN BUTTES NR DEETH	0.02	0.00	0.02	1.00
B	10316500	LAMOILLE CREEK	7.03	2.29	4.74	0.67
C (003)	10318500	HUMBOLDT RV NR ELKO	2.24	0.06	2.18	0.97
D	10320000	SOUTH-FORK-HUMBOLDT RIVER	6.45	2.43	4.02	0.62
E	10321000	HUMBOLDT RV NR CARLIN	13.85	4.91	8.95	0.65
F	10321590	SUSIE CK AT CARLIN	3.61	1.49	2.13	0.40
G	10322000	MAGGIE CK AT CARLIN	11.01	4.47	6.54	0.59
H	10322150	MARYS CK AT CARLIN	6.03	2.14	3.89	0.65
I (004)	10322500	HUMBOLDT RV AT PALISADE	41.55	14.98	26.56	0.64
AVERAGE		UPPER HUMBOLDT RIVER	10.20	3.64	6.56	0.69
K	10323425	HUMBOLDT RV AT OLD US 40 BRG AT DUNPHY	21.14	8.16	12.98	0.61
L	10324500	ROCK CREEK	0.36	0.23	0.12	0.35
M	10324700	BOULDER CREEK	4.60	2.57	2.03	0.44
N	10325000	HUMBOLDT RV AT BATTLE MOUNTAIN	6.80	3.72	3.08	0.45
AVERAGE		MIDDLE HUMBOLDT RIVER	8.22	3.67	4.55	0.46
O (007)	10327500	HUMBOLDT RV AT COMUS	0.31	0.11	0.19	0.64
P	10329000	LITTLE HUMBOLDT RIVER	31.98	11.90	20.08	0.63
Q	10329500	MARTIN CREEK NR PARADISE VALLEY	9.83	3.50	6.33	0.64
V (013)	10333000	HUMBOLDT RV NR IMLAY	10.73	4.31	6.43	0.60
X (016)	10335000	HUMBOLDT RIVER NR RYE PATCH RESERVOIR	527.38	204.38	322.99	0.61
AVERAGE		LOWER HUMBOLDT RIVER	116.05	44.84	71.21	0.62

See Fig. 1 for locations of stream-flow gages with abbreviated IDs

*See Fig. 1 for locations of the stations. (Sample #) corresponds to locations of water sample collection. *BFI* base flow Index: ratio of total base flow to total flow

Results and analysis

Chemistry of water

Table 1 lists physical and chemical composition of the HR waters. In general, the river water is alkaline and oxic with pH 8.64–9.13 and ORP 10–192.4 mV along with conductivity 720–1280 $\mu\text{S}/\text{cm}$. The chemistry of water evolves from (Na + K) – SO₄ type in the UHR and (N + K) – HCO₃ type in the northern LHR to (Na + K) – Cl type in the Lovelock Valley (Fig. 2). See Fig. 3 for Stiff diagrams illustrating the evolution of water chemistry along the flow-path of the river.

Concentrations of As range from 0.012 to 0.066 mg/L with an average of 0.03 mg/L (Table 1). Stable isotopes of the HR water samples range from –7.5 to –15.7‰ for ¹⁸O and from –85 to –125‰ for deuterium. The plot of ¹⁸O versus δD isotopes (Fig. 4) illustrates that overall water has δD and ¹⁸O values that shift from the Craig's GMWL (1961) towards right with a slope of 4.8, implying the process of evaporation (Clark and Fritz 1997; Sueker 2003). Sulfur isotopes of dissolved sulfate range from +4.7

to +12‰ with an average of +8.8‰ (Table 1). While the range of isotopic signatures of $\delta^{34}\text{S}$ and SO₄²⁻ values in this study warrants explanations for variation of dissolved sulfate concentrations along the flow-path of the stream, the dual isotopic signatures of $\delta^{34}\text{S}$ and ¹⁸O values can provide the approximate source of sulfate in the waters. Sulfate derived from dissolution of primary evaporites, for example, has relatively high $\delta^{34}\text{S}$ and ¹⁸O values; whereas, sulfate derived from sulfide oxidation usually has comparatively low $\delta^{34}\text{S}$ and ¹⁸O values (Krouse and Mayer 2000). Increasing sulfate concentrations in samples 001 and 003 with decreasing $\delta^{34}\text{S}$ values may point to pyrite oxidation as a potential sulfate source in the UHR.

Chemistry and mineralogy of riverbed sediments

The XRD analysis of sediments reveals that the most abundant minerals are quartz, orthoclase feldspar, calcite, biotite, and muscovite. See Figs. C.1 and C.2 (in Online Appendix C) for XRD analysis results. SEM analysis of the sediments further identifies silicate and detrital aluminum silicate

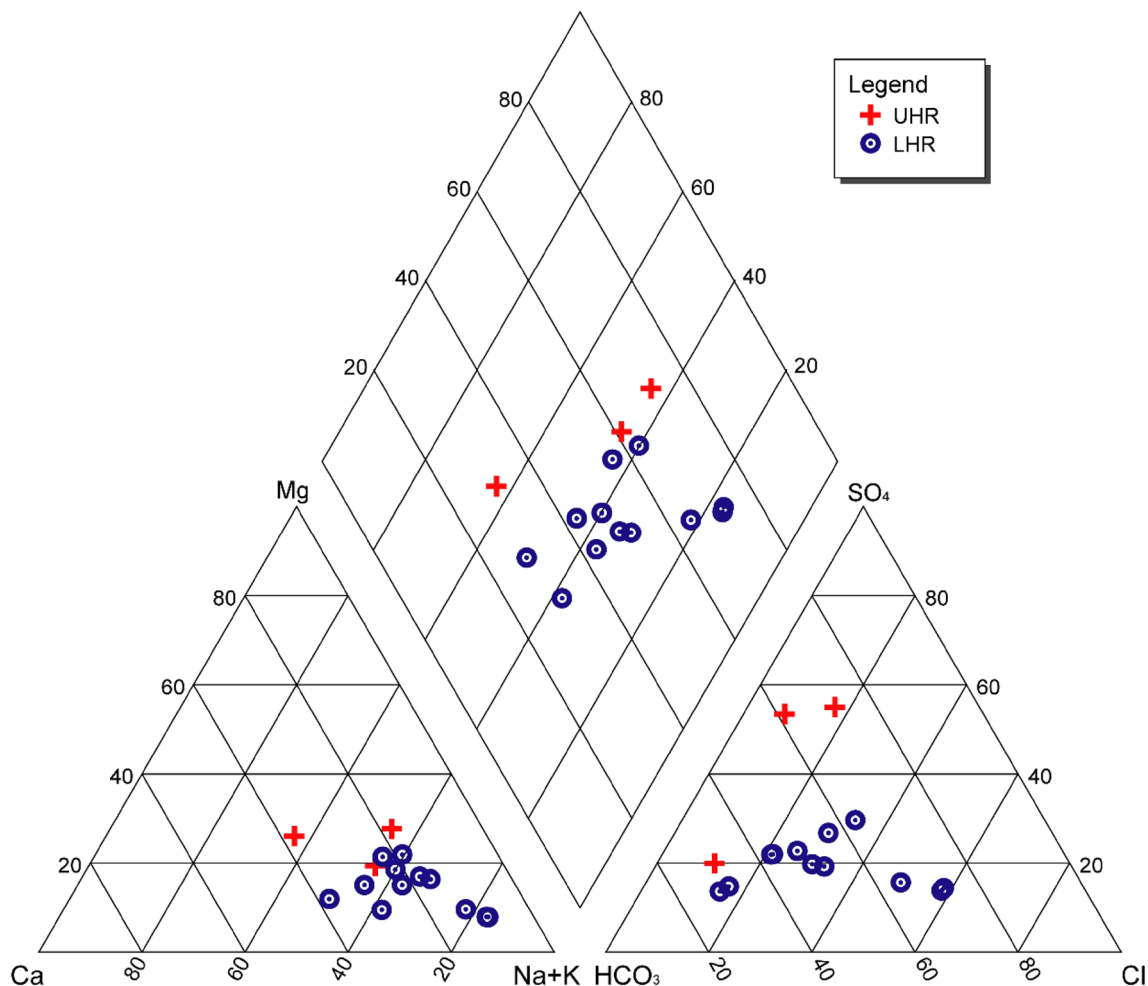


Fig. 2 Piper diagram showing hydro-chemical phases for river waters of the upper, middle and the lower Humboldt River

clay minerals (Fig. 5a–f). Sediment samples 006 and 007 (Fig. 5a, b), for example, illustrate typical flaky texture of detrital smectite clay on the surface of quartz grains. Samples 012 and 015 (Fig. 5c, d), illustrate smectite–illite growth with typical flaky smectite clay minerals on the surface of partially dissolved feldspar. Samples 016 and 019 (Fig. 5e, f) illustrate detrital flaky smectite clays on the surface of partially dissolved feldspar minerals. The EDS in conjunction with SEM analysis results also reveals the presence of ferrihydrite in addition to silicate clay minerals in the riverbed sediments. See Figs. D.1, D.2, and D.3 (in Online Appendix D) for EDS analysis results on a surface of sediment sample showing quantitative elemental composition represented by a spectrum.

Results of sequential extraction analysis for As and other elements in the riverbed sediment samples are provided in Table B.1 (Online Appendix B). Figure 6 illustrates the elemental concentrations of As, Al, Fe, and Ca in percentage to total concentrations of elements in the riverbed sediments. On average, about 83% of total As is extracted from

the residual fraction, which corresponds to silicate and clay minerals. The second most extracted As (13% extraction) is from the Fe–Mn oxide fraction. Arsenic in the organic metal fraction, carbonates, and exchangeable fractions are very low, averaging 1.8%, 0.29% and 0.094%, respectively. The lowest percentages of As from the exchangeable fraction (0.094%) indicate that As is not readily available for exchange.

Aluminum (Al), one of the strongly hydrolyzing elements, is measured almost exclusively (about 64%) in the residual fraction, which is one of the major constituents of clay minerals, and feldspars. Relatively lesser amount of Al detected in carbonates (13%) and organic matter (20%) fractions correspond to Al bound to carbonates and organic matter. The higher percentage of Al in the organic fractions has been well documented in soil chemistry literatures. Curtin (2002), for example, describes that the distribution of organic carbon among the size fractions of soil shows a relationship with Al, because Al has strong inclination to complex with organic matter, what is known as organo-metal

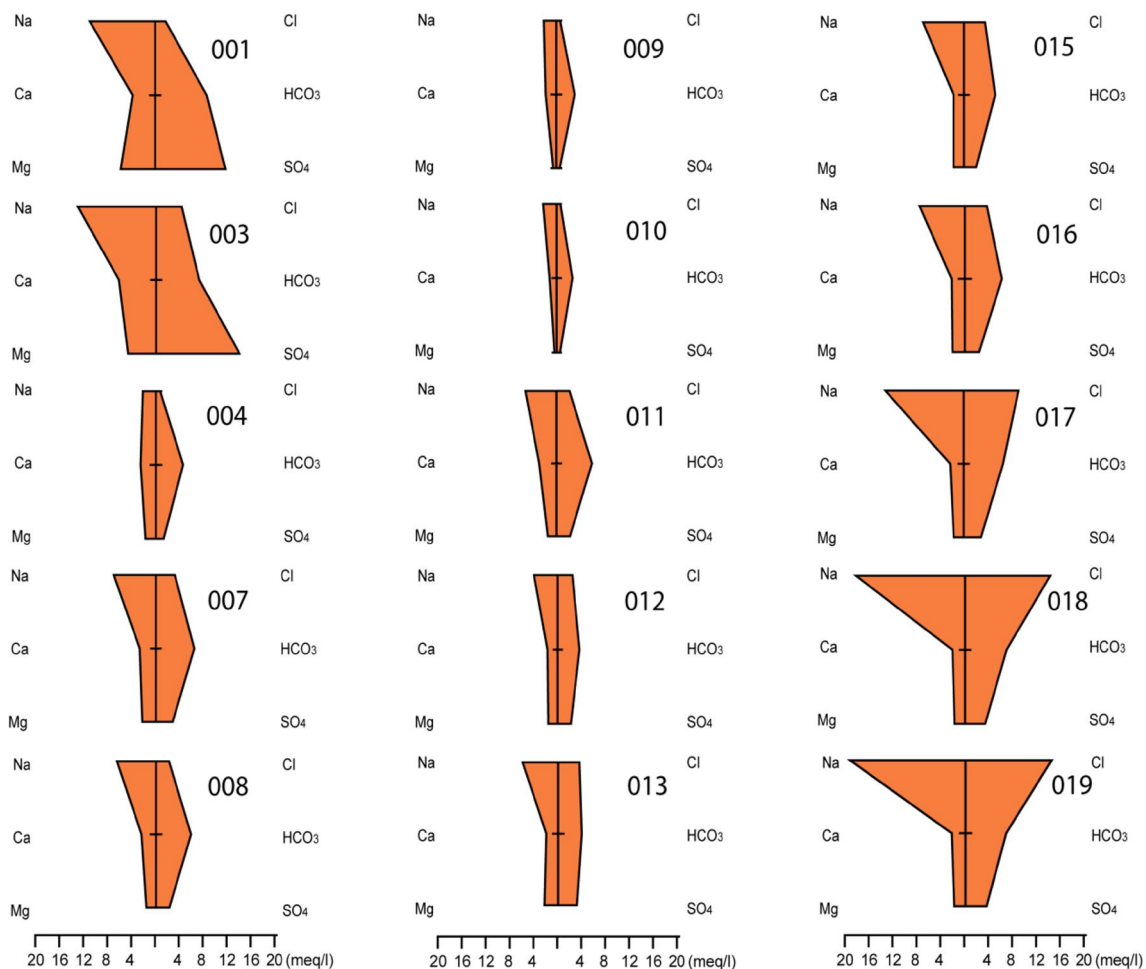


Fig. 3 Stiff diagrams of river water samples (sample numbers on right of each diagram) showing differences in major chemical composition. Samples from the UHR (001 and 003) have high contents

interactions. About 82% of total iron (Fe) is bound to the residual fraction, followed by about 10% to the Fe–Mn oxide fraction, and about 4% to carbonate-bound metal fractions. About 70% of total Ca occurs in the residual fraction, followed by 26% in carbonate fractions.

The relative dominance of Al (64%), Ca (70%), and Fe (82%) in the residual fraction can be accounted for silicate (e.g., feldspars) and clay minerals, such as smectite, and Fe-bearing illite, which have been identified by XRD and SEM analyses. A relatively, lesser amount of Fe (about 10%) in Mn–Fe oxide and hydroxide fraction can be accounted for by Fe partitioned into amorphous and poorly crystalline hydroxides, as observed in the SEM and XRD analyses.

Relationship of arsenic in sediments and waters

Tables 3 and 4 list the results of factor analysis on total elemental concentrations for riverbed sediments. In UHR sediments (samples 001–003), two factors have been identified

of Na–SO₄; samples from 004 to 016 illustrate almost similar composition with Na–HCO₃, whereas samples from 017 to 019 illustrate higher contents of Na–Cl

(Table 3). Factor 1 has strong positive loadings on Al, Ca, Co, Cu, Fe, Ni, but strong negative loading on U and weak positive loading on As (0.3) that represents 63.5% of the total variance. Factor 2 has strong positive loadings on B, Cd, and Mo, and negative loadings on As (–0.95), that represents 36.5% of the total variance. Results suggest that As is associated with Al, Ca, Co, Cu, Fe and Ni, though weakly in majority of the sediment samples in the UHR. On the other hand, As is not associated at all with B, Cd, Mo and U in the UHR sediments. The resulting mineralogy and elemental composition from XRD and SEM using EDS analysis of the UHR sediments generally agrees to the factor analysis results that As and other trace elements, Co, Cu, and Ni are associated with silicate clay minerals and ferrihydrites.

In the LHR sediments (samples 007–019), two factors have been identified (Table 4). Factor 1 has strong positive loadings on Al, As, B, Ca, Cd, Co, Fe, Mo, Ni, and U that represents 75% of the total variance. Factor 2 has negative loading on As (–0.41), that represents 13% of the

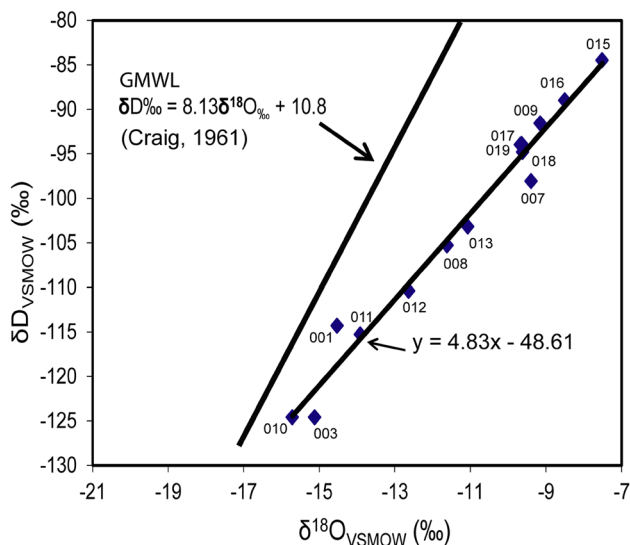


Fig. 4 Relationship between oxygen and hydrogen isotope data of water samples collected from the Humboldt River and its tributaries. The numbers adjacent to each point indicate the corresponding sampling stations

total variance. This suggests that As is strongly associated with Al, B, Ca, Cd, Co, Fe, Mo, Ni and U in the majority (75%) of the LHR sediments. Mineralogical and elemental composition from the XRD and SEM using EDS analysis largely agrees to the factor analysis results that As and other trace elements, B, Cd, Co, Mo, Ni and U are distributed with silicate clay minerals and ferrihydrites.

Factor analysis of the upper and lower HR waters indicates the relative importance of geographic regions in water chemistry and As concentrations in river water. Tables 5 and 6 present these results of factor analysis for river waters. In the UHR waters, dissolved As is moderately associated (0.41) in factor 1 which represents the majority (61.8%) of the total variance with strong loadings on ORP, alkalinity, Ca, Cl, Cu, K, Mg, Na, and SO_4 (Table 6), and reflects oxidation of sulfides with strong positive loading of SO_4 (1.0) and ORP (1.0).

In the LHR, dissolved As is not significant as evidenced by negative factor loading (-0.33) for factor 1 that represents 44% of the variances with strong positive factor loadings on conductivity, B, Ba, Ca, Fe, K, Mg, and Na (Table 6). Moderate factor loading on Cl and high loadings on conductivity, Na, K, Mg, Ca, Ba, and B suggest that the evolved water chemistry in the LHR reflects various processes, including dissolution of minerals, evaporation and/or mixing with geothermal waters. High factor loadings on Al, dissolved SiO_2 and SO_4 , in factor 2 with 19% of the variances probably reflect dissolution of silicates and sulfate salts. Moderate loading on As with high loading on Cl but negative high loading on temperature in factor 3 with 14%

of the variances probably reflects the water chemistry from evaporative enrichment, but not geothermal water mixing. Moderate loading on As with high loading on Li in factor 4 with 11% of the variances probably reflects the water chemistry influenced by mixing with geothermal water, because Li is recognized as a tracer for geothermal waters in this region (Munk et al. 2016).

Discussion

Arsenic in river sediments

The results of sequential extractions illustrate that the highest amount of solid-phase As (83%) is found in the residual fraction, followed by Fe–Mn oxide phases (13%) in all sediment samples (Fig. 6, Table B.1). The results of XRD and SEM analysis with widespread occurrence of feldspar, partially dissolved feldspar, illite, smectite, and quartz (Fig. 5a–f) confirm silicate and aluminum silicate clay minerals in the residual fraction. The results of the sequential extraction analysis of sediments are consistent with the results of factor analysis conducted on the total elemental concentrations of both UHR and LHR bed-sediments (Tables 3 and 4).

The importance of As-bearing iron oxy-hydroxides for widespread natural arsenic occurrence in groundwater has been reported in many parts of the world by and large under reducing condition (Smedley and Kinniburgh 2002; Saunders et al. 2005; Herath et al. 2016). Occurrence of As in Fe–Mn oxides and hydroxides (Folger 2000; Welch et al. 2000) has been reported in the reducing groundwater aquifers close to this study area. However, As in silicate minerals in the river sediments, which is near-surface and oxidizing, has not been reported previously. Nevertheless, the importance of silicate minerals for As has been reported in many similar river flood-plain sediments. Biotite, for example, has been reported for silicate-phase As in many parts of the world (Smedley and Kinniburgh 2002; Charlet et al. 2005; Seddique et al. 2008). Biotite is one of the fastest weathering silicate minerals, and is the most likely source of As from weathering of typical igneous and metamorphic rocks. The above results suggest that silicate mineral phases predominantly control As distribution in the HR sediments. Iron oxy-hydroxide minerals play a lesser degree in controlling As distribution in the HR sediments, which are near-surface and predominantly oxidizing in nature.

Arsenic in river waters

The water samples for this study were collected during low-flow season and therefore, seasonal perturbation of As concentrations in the HR waters was investigated using water quality data from Nevada Division of Environmental

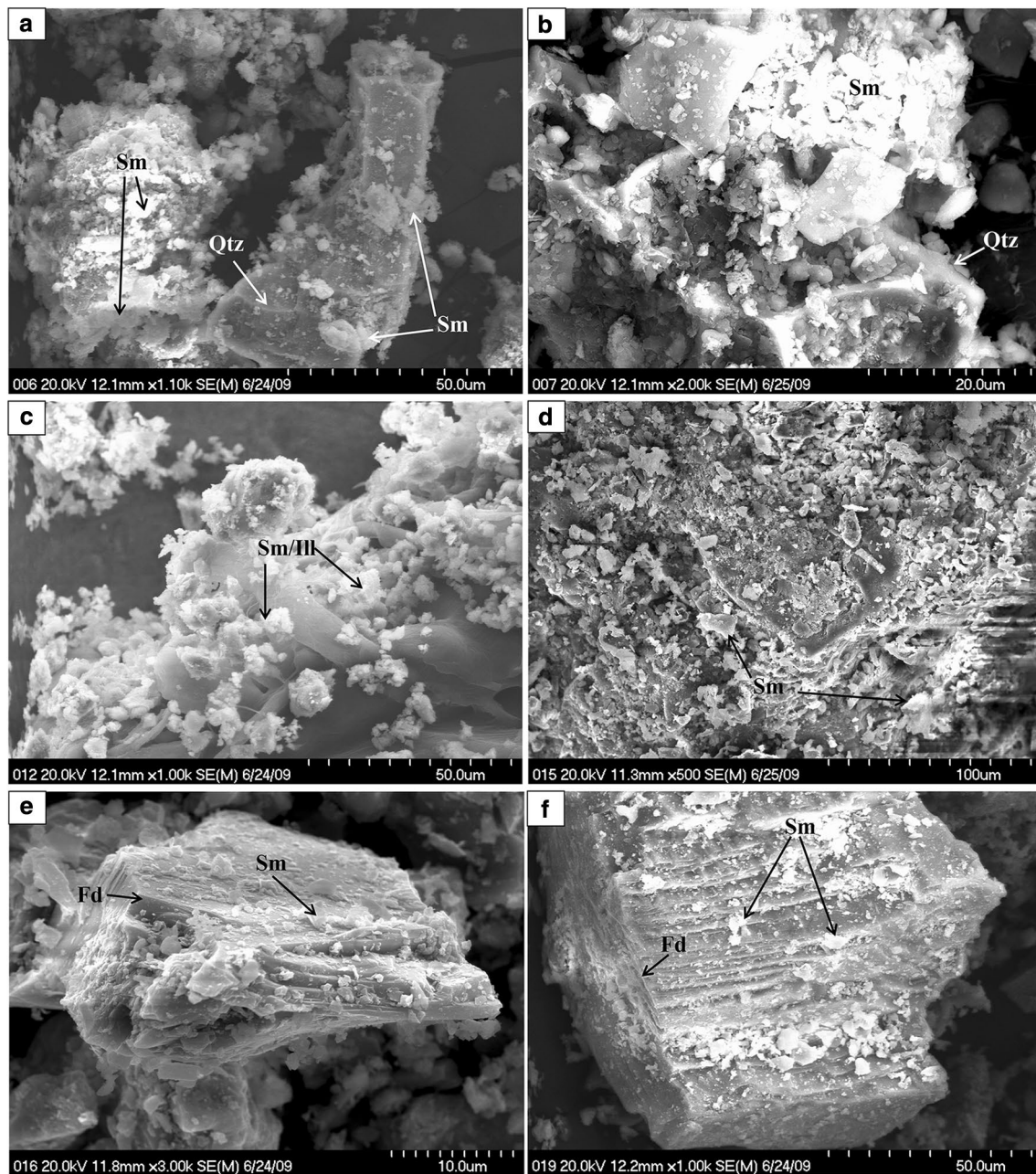


Fig. 5 **a** Photomicrograph of riverbed sediments (sample 006), illustrating typical detrital smectite clay (Sm) on the surface quartz (Qtz) grains. **b** Photomicrographs of riverbed sediments (sample 007), illustrating typical flaky nature of smectite (Sm) clay minerals on the surface of quartz (Qtz) grains. **c** Photomicrographs of riverbed sediments (sample 012), illustrating smectite–illite (Sm/III). **d** Photomicrographs of riverbed sediments (sample 015), illustrating typical

flaky nature of smectite (Sm) clay minerals on the surface of partially dissolved feldspar. **e** Photomicrographs of riverbed sediments (sample 016), illustrating detrital flaky smectite clays (Sm) on the surface of feldspar (Fd). **f** Photomicrographs of riverbed sediments (sample 019), illustrating typical flaky nature of smectite (Sm) clay minerals on the surface of partially dissolved feldspar (Fd)

Protection (NDEP). The data were filtered for the year of 2007 for As and other chemical parameters. The months from March to July are high-flow season, and from August to December are low-flow season. Table E.1 (in Online Appendix E) lists these data with sample locations.

Concentrations of dissolved As reveal little or no variation at various stations despite concentrations of dissolved Cl, SO₄, and TDS vary to a greater degree (Table E.1 in Online Appendix E). In the Maggie Creek (HS14 in Table E.1 in Online Appendix E) of the UHR, for example, As

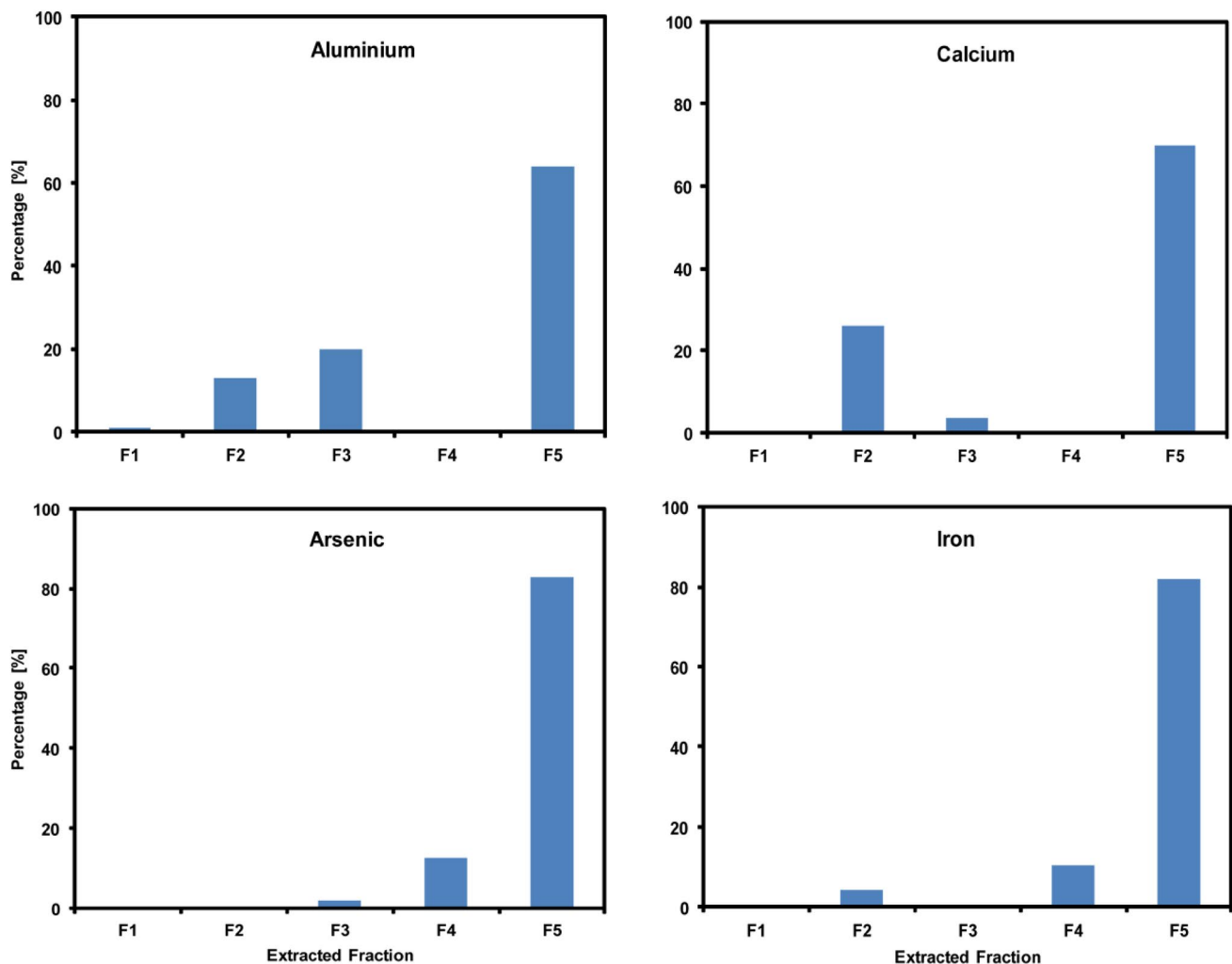


Fig. 6 Elemental concentrations (%) of some key-elements in the riverbed sediments obtained from sequential extraction analyses. F1: Exchangeable fraction; F2: carbonate-bound fraction; F3: organic metal fraction; F4: Fe–Mn oxide and hydroxide fraction; F5: residual fraction

concentrations change marginally from 13 $\mu\text{g/L}$ in high flow season to 18 $\mu\text{g/L}$ (average) in low-flow season. Concentration of As remains the same and so do the values for pH and Cl, but the concentration of SO_4 increases from high-flow to low-flow season for HS15 station in the UHR (Table E.1 in Online Appendix E). On the other hand, no significant change is observed in pH, As, Cl and SO_4 concentrations in stations HS2B and HS3A for North-Fork-Humboldt River and South-Fork-Humboldt River in the UHR. Concentrations of As changed from 7 $\mu\text{g/L}$ in high-flow season to 12 $\mu\text{g/L}$ (average) in low-flow season for HS4 near Cosino in the upstream of Elko. No significant change is observed in As concentration for HS5 in Carlin between August and December.

Significant changes in concentrations of dissolved Cl, SO_4 , and TDS are observed in different seasons in station HS12 above Humboldt Sink in LHR. For example, dissolved Cl concentration changes from 1400 mg/L in April

to 130 mg/L in August, and then to 680 mg/L in December. However, concentrations of As do not change significantly in this station. The higher concentration of Cl in April is due to additional runoffs from the nearby agricultural farmlands and ranches. With the present data, it can be inferred that Cl concentrations in LHR may be affected by seasonal effects and stream-flow conditions; however, As concentrations are not affected significantly. Therefore, changes in As concentrations in different parts of the HR reflect different geochemical and physical processes without significant seasonal perturbations.

Processes in the UHR

The strong positive loading of dissolved SO_4 (1.0) and ORP (1.0) with moderate loading of As (0.41) in the UHR (Table 5) waters suggest moderate importance of oxidative dissolution of As-bearing sulfide minerals as a process. This

Table 3 Factor analysis results of total elemental concentrations of the Upper Humboldt River-bed sediments (samples from 001 to 003) that were digested in aqua-regia

Component	Factor 1	Factor 2	Communalities
Al	1.00	0.05	1
As	0.30	-0.95	1
B	-0.10	1.00	1
Ca	1.00	-0.07	1
Cd	0.01	1.00	1
Co	1.00	-0.04	1
Cu	0.83	0.55	1
Fe	1.00	0.04	1
Mo	-0.51	0.86	1
Ni	1.00	0.10	1
U	-0.98	0.21	1
Initial Eigenvalues	6.99	4.01	
Percentage of variance	63.5	36.5	
Cumulative % of variance	63.5	100	
Total communalities			11
Proportion of the total variation explained by the factors			1

Statistical results were obtained by applying Principal Component Analysis (PCA). The numbers in the rows represent factor loadings for each component, and marked bold typefaces represent the values of factor loadings of over 0.75. Statistics are based on cases with no missing values for any variable used

is consistent with the geologic distribution of As-bearing sulfide minerals and/or rocks (e.g., pyrite, arsenopyrite) along with the presence of several active surface gold mines in the catchment areas of the UHR (Theodore et al. 2003) with prevalent aerobic or oxic conditions. The moderate importance of oxidation of sulfide minerals is best displayed in Figs. 7 and 8, where the excess of SO_4 with respect to Cl in the UHR at samples 001 and 003 can be directly attributed to oxidation of sulfide minerals. In a similar study at North Fork watershed in the UHR region, Earman and Hershey (2004) reported high concentrations of dissolved As (0.016 mg/L) and SO_4 (370 mg/L). They suggested oxidation of mined waste rocks containing As-bearing sulfide minerals as the primary source for high dissolved As and SO_4 in the waters followed by in situ acid neutralization by dissolution of carbonate host rocks.

The sulfur isotopic signatures ($\delta^{34}\text{S}$ of SO_4) also support oxidation of sulfide minerals for the source of dissolved SO_4 in the upstream area. The two upstream samples (001 and 003) with high concentrations of dissolved SO_4 (565 mg/L and 566 mg/L, respectively) with +4.7‰ and +9.8‰ of $\delta^{34}\text{S}$, respectively, are indicative of localized sulfide oxidation in the upstream area.

Table 4 Factor analysis results of total elemental concentrations of the Lower Humboldt River-bed sediments (samples from 007 to 019) that were digested in aqua-regia

Component	Factor 1	Factor 2	Communalities
Al	0.85	0.33	0.83
As	0.82	-0.41	0.84
B	0.89	-0.41	0.96
Ca	0.85	0.32	0.83
Cd	0.86	-0.49	0.97
Co	0.94	0.14	0.90
Cu	0.69	0.45	0.67
Fe	0.94	0.29	0.97
Mo	0.82	-0.52	0.94
Ni	0.91	0.28	0.91
U	0.94	0.02	0.89
Initial Eigenvalues	8.30	1.43	
Percentage of variance	75.45	13.02	
Cumulative % of variance	75.45	88.47	
Total communalities			9.73
Proportion of the total variation explained by the factors			0.88

Statistical results were obtained by applying Principal Component Analysis (PCA). The numbers in the rows represent factor loadings for each component, and marked bold typefaces represent the values of factor loadings of over 0.75. Statistics are based on cases with no missing values for any variable used

The acid neutralization must have occurred following oxidative dissolution of As-bearing sulfide minerals by dissolution of carbonate rocks to reflect the water chemistry in the HR. Intuitively, the relatively high loadings of dissolved Ca, and Mg, with alkalinity (as HCO_3^-) in the UHR waters infer dissolution of carbonate rocks containing limestone and dolomite in the UHR region. Carbonate dissolution is consistent with the occurrence of Pre-Cenozoic carbonate rocks containing limestone and dolomite in northeastern and northern part of the UHR region (Wallace et al. 2004).

The change in dissolved SO_4 concentrations from sample 003 (566.3 mg/L) to sample 004 (59.3 mg/L) in the upstream area can be explained by the coupled effect of dilution/mixing with relatively reduced groundwater, where sample 004 is located in the downstream of the confluence of South Fork-Humboldt River and the HR (Fig. 1). In general, sulfide oxidation reactions can occur in two ways under natural conditions. The first sulfide oxidation occurs by oxygen, where the oxygen in the sulfate is contributed by molecular atmospheric oxygen, resulting in enriched sulfate in the heavy sulfur isotope ($\delta^{34}\text{S}$) and the light oxygen isotope ($\delta^{18}\text{O}$). The second sulfide oxidation occurs by ferric iron, where the oxygen in the sulfate is derived exclusively from water

Table 5 Factor analysis results of total elemental concentrations of the Upper Humboldt River-waters (samples from 001 to 004) that were digested in aqua-regia

Component	Factor 1	Factor 2	Communalities
pH	-0.84	0.55	1
ORP	1.00	0.02	1
Cond	0.49	0.87	1
Temp	-0.21	-0.98	1
Alk	0.92	0.40	1
Al	0.57	-0.82	1
As	0.41	0.91	1
B	0.69	0.73	1
Ba	0.16	0.99	1
Ca	0.82	-0.57	1
Cl	1.00	0.08	1
Cu	1.00	0.08	1
Fe	-1.00	-0.08	1
K	0.98	0.19	1
Li	0.57	-0.82	1
Mg	0.94	0.33	1
Mn	0.47	-0.88	1
Na	1.00	-0.10	1
SiO ₂	0.71	-0.71	1
SO ₄	1.00	0.08	1
Initial Eigenvalues	12.4	7.64	
Percentage of variance	61.8	38.2	
Cumulative % of variance	61.8	100	
Total communalities			20
The proportion of the total variation explained by the factors			1

Statistical results were obtained by applying Principal Component Analysis (PCA). The numbers in the rows represent factor loadings for each component, and marked bold typefaces represent the values of factor loadings of over 0.75. Statistics are based on cases with no missing values for any variable used

ORP oxidation–reduction potential, Cond conductivity, Temp temperature, Alk alkalinity

resulting in light oxygen isotope ($\delta^{18}\text{O}$) (Liu et al. 2017). Decreasing sulfate concentration from samples 001 and 003 to sample 004 with increasing $\delta^{34}\text{S}$ and $\delta^{18}\text{O}$ values are indicative for dissimilatory bacterial sulfate reduction (Krouse and Mayer 2000). The sharp reduction in dissolved SO_4 is accompanied by sharp reduction in ORP from 134 to 10 mV with increase in dissolved Fe concentration from < 0.01 to 0.019 mg/L from sample 003 to sample 004 (Table 1). The solubility of Fe^{2+} is greater than that of Fe^{3+} at relatively reduced or less oxic conditions. Therefore, decrease in dissolved As and SO_4 from sample 001 and 003–004 is primarily due to mixing with relatively reduced ground water as evidenced by base flow analysis and stream-flow data (Table 2).

Processes in the LHR

Factor analysis results for the LHR waters reveal that, dissolved As is not significant in factor 1 with negative factor loading (-0.33) that represents 44% of the variances with strong positive factor loadings on conductivity, B, Ba, Ca, Fe, K, Mg, and Na (Table 6). Factor 2 with 19% of the variances have high factor loadings on Al, dissolved SiO_2 and SO_4 , and negative factor loading for As (-0.26), which reflects dissolution of silicates and sulfates. Factor 3 represents 14% of the variances and hence, only 14% of water from the LHR represent the processes of evaporation because of positive loadings for As (0.64) and Cl (0.78) and negative loading for temperature (-0.90). Mixing of geothermal water is inferred for only 12% of water represented by factor 4, with positive loading for Li (0.78) and As (0.52). This is suggested because, (1) several geothermal hot springs are active in the vicinity, such as in Golconda; and (2) dissolved Li is recognized as tracers for geothermal waters in this area (Munk et al. 2016). See Table F.1 (in Online Appendix F) for groundwater quality data in Golconda. However, relatively lower concentrations of dissolved As (mean 0.01 mg/L) in the Golconda hot spring system, and relatively higher As concentrations in samples 007 and 008 (0.021 mg/L and 0.037 mg/L, respectively) near Golconda invokes inputs other than thermal spring waters. The BFI near Golconda is 0.45–0.64 indication base flow with 45–64%, respectively, and hence the change in As concentration is most likely due to ground water discharge to the HR in this site.

In the southern part of LHR region, evaporation is inferred with positive correlations between As and Cl (sample 015–019 in Table 1). Analysis of PET data combined with stable isotope data suggests evaporation as the most likely process for excess of Cl and other dissolved ions. Statewide PET data (Table A.2 in Online Appendix A) suggest that average annual PET rates are higher than precipitation in Imlay, where dissolved As and Cl increases slightly (Table 1) from sample locations 011–012. Concentrations of dissolved As increase from 0.02 mg/L at sample 013 near Imlay to 0.048 mg/L at sample 015 near Rye Patch Reservoir Dam along with increases in dissolved Cl. These consistent increases in Cl and As are inferred due to evaporation based on stable isotope data and PET data in the area. A minor fluctuation with decrease in dissolved Cl, SO_4 and As from samples 015–016 can be explained by dilution from additional flow of water from the reservoir. Concentration of dissolved As incrementally increases downstream of sample location 016 towards sample locations 017, 018 and 019 in the Lovelock Valley (Table 1). The increase in dissolved As along with Cl and other ions are due to progressive evaporative enrichment of the HR water.

Table 6 Factor analysis results of total elemental concentrations of Lower Humboldt River-waters (samples from 007 to 019) that were digested in aqua-regia

Component	Factor 1	Factor 2	Factor 3	Factor 4	Communalities
pH	0.25	-0.86	-0.31	0.02	0.90
ORP	-0.40	-0.16	0.45	-0.64	0.80
Cond	0.95	-0.10	-0.03	0.09	0.92
Temp	0.29	-0.04	-0.90	0.26	0.96
Alk	0.56	0.73	-0.10	0.29	0.93
Al	-0.30	0.91	0.10	0.17	0.96
As	-0.33	-0.26	0.64	0.52	0.86
B	0.96	0.14	0.19	-0.12	0.98
Ba	0.97	-0.02	-0.03	-0.16	0.98
Ca	0.93	0.08	0.27	-0.20	0.99
Cl	0.56	0.11	0.78	-0.03	0.93
Cu	0.55	0.09	0.22	0.22	0.40
Fe	0.91	-0.19	-0.33	-0.06	0.97
K	0.83	0.00	0.36	-0.35	0.95
Li	0.23	0.30	0.04	0.78	0.75
Mg	0.92	-0.18	-0.03	0.12	0.90
Mn	0.33	-0.03	0.35	0.60	0.60
Na	0.94	0.03	-0.15	-0.18	0.93
SiO ₂	-0.39	0.82	-0.10	-0.30	0.92
SO ₄	0.38	0.83	-0.26	-0.27	0.97
Initial Eigenvalues	8.75	3.77	2.78	2.29	
Percentage of variance	43.8	18.9	13.9	11.5	
Cumulative % of variance	43.8	62.6	76.5	88.0	
Total communalities					17.6
The proportion of the total variation explained by the factors					0.88

Statistical results were obtained by applying Principal Component Analysis (PCA). The numbers in the rows represent factor loadings for each component, and marked bold typefaces represent the values of factor loadings of over 0.75. Statistics are based on cases with no missing values for any variable used

ORP oxidation–reduction potential, Cond conductivity, Temp temperature, Alk alkalinity

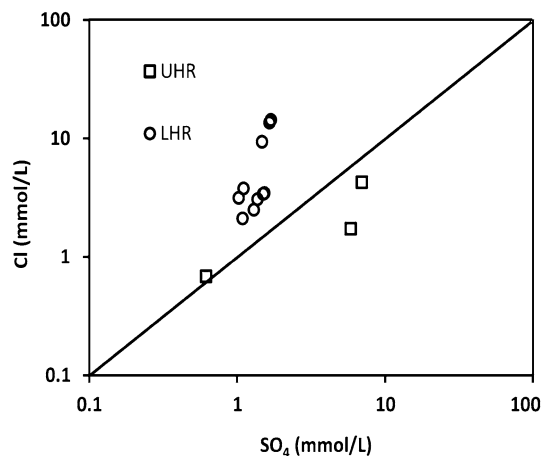


Fig. 7 Sulfate concentrations (in mmol/L) vs. Chloride concentrations (mmol/L) in water samples from the Humboldt River

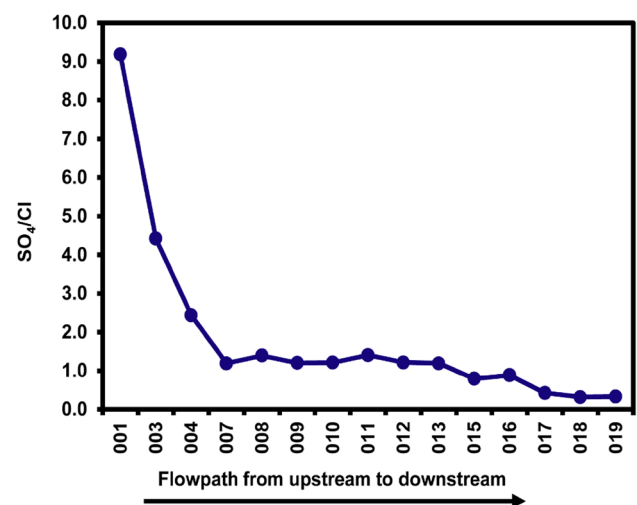


Fig. 8 Ratio of dissolved sulfate to chloride in the waters along the flow-path of the Humboldt River. Ratio of sulfate to chloride gradually decreases in the LHR

The enrichment of deuterium and O-18 (Fig. 4) of the waters in the southern part of the LHR, especially samples from 015 to 019, suggests that evaporation is an important process in these waters. The importance of evaporation in the LHR is best illustrated in Figs. 7 and 8. In these figures, the ratio of SO_4 to Cl is higher in the UHR because of excess of dissolved SO_4 with respect to Cl as a result of more dissolved SO_4 from oxidation of sulfide minerals, but the ratio SO_4/Cl gradually becomes less than one in the LHR because of gradual increase in Cl due to evaporation.

In many oxidizing systems such as in Carson Sink, located in the vicinity of Humboldt Sink in Western US (Welch et al. 2000), pH is positively correlated with dissolved As, and elevated concentrations of As has been linked to pH-dependent desorption. The HR water is alkaline with pH ranges from 8.44 to 9.25. At alkaline pH, mineral surfaces become increasingly negatively charged, and thus promote arsenic desorption. However, the effect of pH in secondary As enrichment remains inconclusive because of the lack of correlations in all waters from UHR to LHR.

Conclusions

The study concludes that concentrations of As in the HR waters and sediments are controlled by several geochemical and hydrological processes. The findings from this study are summarized below.

1. Oxidation of As-bearing sulfide minerals from metal-ore deposits is the primary source for dissolved As in the upper HR locally because of the prevalent oxidizing environment with widespread availability of sulfide minerals in the region. The process of oxidative dissolution becomes less significant along the flow-path towards the middle and lower HR.
2. Subsequent mixing of river water with discharging groundwater results in dilution of As and SO_4 in the waters towards the middle HR.
3. Localized mixing of geothermal and As-rich groundwater increases dissolved As concentrations in the waters in the lower HR near Golconda.
4. Subsequent enrichment of dissolved As occurs from evaporative enrichment of the river water in the lower reaches because of the favorable arid and temperate climate with widespread surface areas around the terminal sink in the lower HR.
5. Arsenic distribution in the river sediments is controlled by partitioning primarily onto silicate clay minerals followed by Fe-oxy-hydroxide minerals in this near-surface oxidizing environment. This implies the risk for potential immobilization of arsenic in groundwater with change in geochemical conditions to reducing conditions

and therefore warrants future studies on groundwater-As geochemical investigation in the HRB.

6. Groundwater–surface water interactions play an important role in dissolved As and other chemical constituent's concentrations. This demonstrates important implication for other naturally occurring chemical constituents in similar arid and semi-arid low-flow river basins and warrants future investigation.

Acknowledgements We would like to acknowledge the contribution of Dr. Simon Poulson at Nevada Stable Isotope Laboratory at the Mackay School of Earth Sciences and Engineering (MSESE) of University of Nevada, Reno (UNR) for his help with the stable isotope analysis. We acknowledge the contribution of Dr. Paul J Lechler at Nevada Bureau of Mines and Geology for his help with the ICPMS analysis of total elements. We thank to the Department of Chemical and Metallurgical Engineering laboratory at UNR for EDS analysis of the sediments using SEM. We truly appreciate Dr. James W. LaMoreaux for editorial handling and reviewer's comments to improve the manuscript.

Funding Funding for the laboratory analysis was provided by the grant to the PI by the University of Nevada, Reno. Funding for fieldwork and sample collection was provided by the Geological Society of America Student grant.

References

- Carmody RW, Plummer LN, Busenberg E, Coplen TB (1998) Methods for collection of dissolved sulfate and sulfide and analysis of their sulfur isotopic composition. US Geol Surv Open File Rep 97–234:91. <https://doi.org/10.3133/ofr97234>
- Charlet L, Chakraborty S, Varma S, Tournassat C, Wolthers M, Chatterjee D, Roman Ross G (2005) Adsorption and heterogeneous reduction of arsenic at the phyllosilicate–water interface. In: Day O', Peggy A, Vlassopoulos D, Meng X, Benning LG (eds) *Advances in arsenic research*. American Chemical Society, Washington, DC, pp 41–59. <https://doi.org/10.1021/bk-2005-0915.ch004>
- Clark I, Fritz P (1997) *Environmental isotopes in hydrogeology*. CRC Press, New York, p 328
- Curtin D (2002) Possible role of aluminum in stabilizing organic matter in particle size fractions of Chernozemic and Solonchic soils. *Can J Soil Sci* 82(2):265–268. <https://doi.org/10.4141/S01-035>
- Davis JC (2002) *Statistics and data analysis in geology*, 3rd edn. Wiley, New York
- Dongarrà G, Manno E, Sabatino G, Varrica D (2009) Geochemical characteristics of waters in mineralised area of Peloritani Mountains (Sicily, Italy). *Appl Geochem* 24:900–914
- Earman S, Hershey RL (2004) Water quality impacts from waste rock at a Carlin-type gold mine, Elko County, Nevada. *Environ Geochem* 45:1043–1053
- Epstein S, Mayeda T (1953) Variation of O^{18} content of waters from natural sources. *Geochim Cosmochim Acta* 4(5):213–224. [https://doi.org/10.1016/0016-7037\(53\)90051-9](https://doi.org/10.1016/0016-7037(53)90051-9)
- Folger HW (2000) Analytical results and sample locations of reanalyzed NURE stream-sediment and soil samples for the Humboldt River Basin mineral-environmental resource assessment, northern Nevada. USGS Open File Report 00-421, US Geological

- Survey, Reston, Virginia. <https://pubs.usgs.gov/of/2000/of00-421>. Accessed 1 Mar 2019
- Herath I, Vithanage M, Bundschuh J, Maity JP, Bhattacharya P (2016) Natural arsenic in global groundwaters: distribution and geochemical triggers for mobilization. *Curr Pollut Rep* 2(1):68–89. <https://doi.org/10.1007/s40726-016-0028-2>
- IBM Corp. Released 2012. IBM SPSS Statistics for Windows, Version 21.0. Armonk, NY: IBM Corp.
- Jang C-S (2010) Applying scores of multivariate statistical analyses to characterize relationships between hydrochemical properties and geological origins of springs in Taiwan. *J Geochem Explor* 105:11–18
- Johannesson KH, Lyons WB, Huey S, Doyle GA, Swanson EE, Hackett E (1997) Oxyanion concentrations in Eastern Sierra Nevada Rivers-2. Arsenic and Phosphate. *Aquat Geochem* 3:61–97
- Krouse HR, Mayer B (2000) Sulphur and oxygen isotopes in sulfate. In: Cook PG, Herczeg AL (eds) *Environmental tracers in subsurface hydrology*. Kluwer, Boston, pp 195–231
- Li X, Coles BJ, Ramsey MH, Thornton I (1995) Sequential extraction of soils for multielement analysis by ICP-AES. *Chem Geol* 124:109–123
- Liu J, Li S, Zhong J, Zhu X, Guo Q, Lang Y, Han X (2017) Sulfate sources constrained by sulfur and oxygen isotopic compositions in the upper reaches of the Xijiang River, China. *Acta Geochim* 36(4):611
- Morrison J, Brockwell T, Merren T, Fourel F, Phillips AM (2001) On-line high-precision stable hydrogen isotopic analyses on nanoliter water samples. *Anal Chem* 73:3570–3575
- Munk L, Hynek S, Bradley DC, Boutt D, Labay KA, Jochens H (2016) Lithium brines: a global perspective. In: Verplanck PL, Hitzman MW (eds) *Rare earth and critical elements in ore deposits, reviews in economic geology*, vol 18, Society of Economic Geologists, Littleton, pp 339–365. <https://pubs.er.usgs.gov/publication/70104988>. Accessed 1 Mar 2019
- NCEI: National Center for Environmental Information (2019) National Oceanic and Atmospheric Administration <https://www.ncdc.noaa.gov/>. Accessed 1 Mar 2019
- Prudic DE, Niswonger RG, Harrill JR, Wood JL (2007) Streambed infiltration and ground-water flow from the Trout Creek drainage, an intermittent tributary to the Humboldt River, north-central Nevada. In: Stonestrom DA, Constantz J, Ferre TPA, Leake SA (eds) *Ground-water recharge in the arid and semiarid southwestern United States*, US Geological Survey Professional Paper 1703-K, Reston, Virginia, pp 313–351. <http://pubs.usgs.gov/pp/pp1703/k>. Accessed 1 Mar 2019
- Reyment RA, Joreskog K (1996) *Applied Factor analysis in the natural sciences*, 2nd edn. Cambridge University Press, Cambridge, p 383
- Saunders JA, Lee M-K, Uddin A, Mohammad S, Wilkin RT, Fayek M, Korte NE (2005) Natural arsenic contamination of Holocene alluvial aquifers by linked tectonic, weathering, and microbial processes. *Geochem Geophys Geosyst* 6(4):Q04006. <https://doi.org/10.1029/2004GC000803>
- Seddique AA, Masuda H, Mitamura M, Shinoda K, Yamanaka T, Itai T, Maruoka T, Uesugi K, Ahmed KM, Biswas DK (2008) Arsenic release from biotite into a Holocene ground water aquifer in Bangladesh. *Appl Geochem* 23(8):2236–2248
- Shelton LR (1994) Field guide for collecting and processing stream-water samples for the national water-quality assessment program. US Geological Survey Open-File Report, pp 94–455. <https://water.usgs.gov/nawqa/pnsp/pubs/ofr94-455/sw-t.html>. Accessed 1 Mar 2019
- Smedley PL, Kinniburgh DG (2002) A review of the source, behaviour and distribution of arsenic in natural water. *Appl Geochem* 17:517–568
- SNDWR: State of Nevada Division of Water Resources (2019). <http://water.nv.gov/EvapotranspirationBasinStation.aspx>. Accessed 20 Aug 2019
- Sueker JK (2003) Isotope applications in environmental investigations part II: groundwater age dating and recharge processes, and provenance of sulfur and methane. *Remediation* 13:71–90. <https://doi.org/10.1002/rem.10065>
- Tessier A, Campbell PGC, Bisson M (1979) Sequential extraction procedure for the speciation of particulate trace metals. *Anal Chem* 51(7):844–851. <https://doi.org/10.1021/ac50043a017>
- Theodore TG, Kotlyar BB, Singer DA, Berger VI, Abbott EW, Foster AL (2003) Applied geochemistry, geology, and mineralogy of the northernmost Carlin Trend, Nevada. *Econ Geol* 98:287–316
- Wallace A, Ludington S, Mihalasky MJ, Peters SG, Theodore TG, Ponce DA, John DA, Berger BR (2004) Assessment of metallic resources in the Humboldt River Basin, Northern Nevada with a section on platinum-group-element (PGE) potential of the Humboldt Mafic Complex. In: Zientek, Michael L, Sidder, Gary B, Zierenberg RA (eds) *US Geological Survey Bulletin 2218*, p 312. <http://pubs.usgs.gov/bul/b2218/>. Accessed 1 Mar 2019
- Wang S-W, Liu C-W, Jang C-S (2007) Factors responsible for high arsenic concentrations in two ground water catchments in Taiwan. *Appl Geochem* 22:460–476
- Web Based Hydrograph Analysis Tool (2019). <https://engineering.purdue.edu/mapserve/WHAT/>. Accessed 1 Mar 2019
- Welch AH, Westjohn DB, Helsel DR, Wanty RB (2000) Arsenic in ground water of the United States: occurrence and geochemistry. *Ground Water* 38:589–604

Publisher's Note Springer Nature remains neutral with regard to jurisdictional claims in published maps and institutional affiliations.